Journal of Molecular Structure 973 (2010) 152–156

Contents lists available at ScienceDirect

Journal of Molecular Structure

journal homepage: www.elsevier.com/locate/molstruc

Crystal X-ray diffraction guided NMR analysis of 3,9-diaryl-2,4,8,10-tetraoxaspiro[5.5]undecanes under differently shielding effect of terminal aromatic rings

Xiaoqiang Sun *, Shu-Ling Yu, Zheng-Yi Li, Yang Yang

Key Laboratory of Fine Petrochemical Engineering, Jiangsu Polytechnic University, Changzhou 213164, Jiangsu, China

ARTICLE INFO

Article history:
Received 29 January 2010
Received in revised form 23 March 2010
Accepted 24 March 2010
Available online 27 March 2010

Keywords:
Spiro-1,3-dioxanes
Pentaerythritol diacetals
Stereoscopic structure
NMR
Crystal X-ray diffraction
Shielding effect

ABSTRACT

The stereoscopic structures of 3,9-di(*o*-, *m*- and *p*-chlorophenyl)-2,4,8,10-tetraoxaspiro[5.5]undecanes were elucidated via high-resolution 1D and 2D NMR techniques including ^{1}H NMR, ^{13}C NMR, DEPT, ^{1}H-^{1}H COSY, HSQC, and HMBC. Complete and accurate assignment of ^{1}H and ^{13}C spectral data, especially the discrimination of hydrogens and carbons in four methylenes under differently shielding effect of aromatic rings were achieved by NMR analysis guided by crystal X-ray diffraction.

1. Introduction

Owing to the characteristic axial and helical chirality, the stereochemistry of spiranes with six-membered rings has been extensively studied [1]. In the past three decades, most of these investigations were carried out with spiranes containing 1,3-dioxane units [1–15]. The chirality of the parent spiro[5.5]undecane was first observed by Dodziuk [4,5] and confirmed by Grosu [6,7]. NMR plays an important role in structural identification, and 2D NMR technique as one of the most effective methods for the determination of molecular spatial structure has been widely used in stereochemistry [16–18]. Although several studies on the stereochemistry of 3,9-disubstituted 2,4,8,10-tetraoxaspiro[5.5]undecane derivatives based on NMR experiments have been well established [2,5,12,13,15], most of them focused on the effect of different substituents such as alkyl and phenyl on position 3,9. Therefore, complete and accurate assignment of proton and carbon signals in four methylenes under the differently shielding effect of terminal aromatic rings is also an interesting challenge. Herein three examples including *o*-, *m*- and *p*-chlorophenyl substituted 2,4,8,10-tetraoxaspiro[5.5]undecanes **1**–**3** (Fig. 1) were investigated respectively to describe the stereochemistry of pentaerythritol diacetals under the differently shielding effect of terminal aromatic rings by 1D and 2D NMR techniques and stereoscopic structure analysis guided by crystal X-ray diffraction.

2. Experimental

2.1. Reagents and samples

All reagents were of analytical grade unless otherwise stated.

Three white compounds **1**–**3** were prepared by the following method. To a solution of *o*-, *m*-, and *p*-chlorobenzaldehyde (5 mmol) and pentaerythritol (3 mmol, 0.41 g) in toluene (25 mL), phosphotungstic acid (1 mol%, 16.5 mg) as catalyst was added, respectively. The mixtures were refluxed for 6–8 h to complete the reaction. After reaction, the mixtures were allowed to cool to the room temperature, and dichloromethane (25 mL) was added to dissolve the product. The insoluble residues were filtrated out and the filtrate was dried over Na_2SO_4. The crude products were isolated by removing CH_2Cl_2 under vacuum to give a white solid in 72%, 63%, and 46% yield, respectively. The pure samples of **1**–**3** for NMR experiments were obtained by recrystallization using ethanol as the solvent.

2.2. NMR measurements

All 1D (^{1}H and ^{13}C) and 2D NMR experiments were performed on a Bruker AVANCE III-500 NMR spectrometer (500.13 MHz for

* Corresponding author. Address: School of Chemistry and Chemical Engineering, Jiangsu Polytechnic University, Changzhou 213164, China. Tel.: +86 (519) 86330003; fax: +86 (519) 86330257.
E-mail address: chemsxq@yahoo.com.cn (X. Sun).

0022-2860/$ - see front matter © 2010 Elsevier B.V. All rights reserved.
doi:10.1016/j.molstruc.2010.03.062

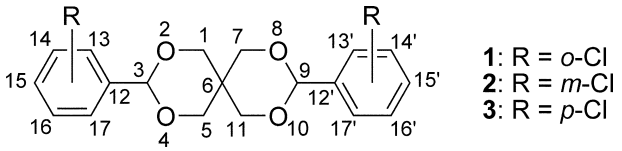

Fig. 1. Structure of 2,4,8,10-tetraoxaspiro[5.5]undecane derivatives **1**–**3**.

^{1}H and 125.77 MHz for ^{13}C) equipped with a 5 mm BBO probe. The specimens were dissolved in 0.5 mL $CDCl_3$, ^{1}H NMR and ^{13}C NMR spectra were recorded on NMR spectrometer using TMS as an internal reference. Chemical shifts (δ) were reported in parts per million (ppm), The pulse conditions were as follows: for the ^{1}H NMR spectrum, spectrometer frequency (SF) = 500.13 MHz, acquisition time (AQ) = 1.638 s, number of scans (NS) = 2, number of dummy scans (DS) = 0, relaxation delay (RD) = 1.0 s, 90° pulse width (PW) = 12.56 μs, spectral width (SW) = 19.99 Hz, Fourier transform (FT) size TD = 32 K; for the ^{13}C NMR spectrum, SF = 125.77 MHz, AQ = 1.10 s, NS = 2048, DS = 4, RD = 1.0 s, 90° pulse width = 9.70 μs, SW = 236.64 Hz, line broadening (LB) = 1.0 Hz, TD = 32 K; for the HSQC spectrum, AQ = 0.051 s, NS = 8, DS = 16, RD = 1.5 s, SW = 19.99 (^{1}H) and 236.64 (^{13}C) Hz, FT size = 1024 × 1024, and 135 Hz one-bond coupling constant; for the HMBC spectrum, AQ = 0.205 s, NS = 8, DS = 16, RD = 1.5 s, F_1 = 29761.91 Hz, F_2 = 5500 Hz, FT size = 2048 × 1024; for the COSY spectrum, AQ = 0.15 s, NS = 4, DS = 4, RD = 1.49 s, F_1 = 6684.49 Hz, F_2 = 6684.49 Hz, FT size = 1024 × 1024, experiment was performed at 298 K.

2.3. X-ray crystallography

M = 381.23, $C_{19}H_{18}Cl_2O_4$, Orthorhombic, Space group $P2_12_12_1$, a = 7.0400(5) Å, b = 7.2389(6) Å, c = 34.674(3) Å, $\alpha = \beta = \gamma = 90°$, V = 1767.1(2) Å^3, Z = 4, D_{calcd} = 1.433 g/cm^3. A colorless crystal of dimension 0.21 × 0.21 × 0.16 mm for compound **1** was used for measurement at 295 (2) K with the φ- and ω-scans mode on a Bruker APEX-II diffractometer with CCD detector using Mo Kα radiation (λ = 0.71073 Å). The data were corrected for Lorentz and polarization effects and absorption corrections based on the multi-scan method were performed using SADABS program. The structure was solved by direct methods and refined by full matrix least-squares methods on F^2 using the SHELXS-97 [19] and SHELXL-97 [20] programs. The positions of hydrogen atoms were calculated theoretically and included in the final cycles of refinement in a riding model along with attached carbons. The final cycle of full matrix least-squares refinement was based on 3447 independent reflections [$I > 2\sigma$ (I)] and 226 variable parameters with R_1 = 0.0377, wR_2 = 0.1142. CCDC 752853 contains the supplementary crystallographic data for this paper. These data can be obtained free of charge via http://www.ccdc.cam.ac.uk/conts/retrieving.html (or from the Cambridge Crystallographic Data Centre, 12, Union Road, Cambridge CB2 1EZ, UK; fax: +44 1223 336033; e-mail: deposit@ccdc.cam.ac.uk).

3. Results and discussion

3.1. Characterization of pentaerythritol diacetals *1*–*3* by 1D and 2D NMR techniques

^{1}H spectra and the ^{13}C spectra for compounds **1**–**3** were measured at room temperature and the results were summarized in Tables 1–3, respectively. $CDCl_3$ was used as solvent for three samples, which provided clear ^{1}H and ^{13}C NMR spectra for **1**–**3**, and most of their signals were resolved. This allowed us to observe the chemical shifts and measure the coupling constants in most cases. Most ^{13}C signals could be assigned through HSQC. For quaternary carbons, analysis of HMBC data was sufficient to complete the assignment.

3.2. Crystal structure of 3,9-di(o-chlorophenyl)-2,4,8,10-tetraoxaspiro[5.5]undecane *1*

A high-quality single crystal of di(*o*-chlorophenyl)-2,4,8,10-tetraoxaspiro[5.5]undecane **1** with *aS* configuration suitable for X-ray crystallography was hazardously picked up from the racemic mixtures of crystals in methanol solution without any chiral separation, which is like in the known experiment of Pasteur. As shown in Fig. 2, the two six-member *O*-heterocycles both adopt chair conformation, and the aromatic rings located at the equatorial of position 3 and 9, which is conformed to the reported similar crystal structures [21,22]. A 2D-net structure packing along *a* and *b* axis

Table 1
^{1}H and ^{13}C NMR chemical shifts, υ (ppm), multiplicities and coupling constants, J (H–H) (Hz), ^{1}H–^{1}H and ^{1}H–^{13}C correlations in HMBC, COSY and HSQC spectra for compound **1**.

C	δC (ppm)	H	δH (ppm)	HMBC	COSY	HSQC
1	70.7 (t)	1	e 3.88 (2H, dd, J = 11.5 Hz, J = 2.5 Hz,) a 3.75 (2H, d, J = 11.5 Hz)	C-3,5,6,7,11	H_a-1, H_e-5 H_e-1	H_a-1, H_e-1
3	99.4 (d)	3	5.84 (2H, s)	C-1,5,13,17	–	H-3
5	71.3 (t)	5	e 4.95 (2H, dd, J = 11.5 Hz, J = 2.5 Hz) a 3.95 (2H, d, J = 11.5 Hz)	C-1,3,6,7,11	H_a-5, H_e-1 H_e-5	H_a-5, H_e-5
6	32.5 (s)	–	–	–	–	–
7	71.3 (t)	7	e 4.95 (2H, dd, J = 11.5 Hz, J = 2.5 Hz) a 3.95 (2H, d, J = 11.5 Hz)	C-1,5,6,9,11	H_a-7, H_e-11 H_e-7	H_a-7, H_e-7
9	99.4 (d)	9	5.84 (2H, s)	C-7,11,13′,17′	–	H-9
11	70.7 (t)	11	e 3.88 (2H, dd, J = 11.5 Hz, J = 2.5 Hz) a 3.75 (2H, d, J = 11.5 Hz)	C-1,5,6,7,9	H_a-11, H_e-7 H_e-11	H_a-11, H_e-11
12	132.6 (s)	–	–	–	–	–
13	135.2 (s)	–	–	–	–	–
14	130.3 (d)	14	7.35 (2H, d)	C-12,13,15,16	H-15	H-14
15	129.5 (d)	15	7.40 (2H, t)	C-13,14,16,17	H-14,16	H-15
16	127.0 (d)	16	7.34 (2H, m)	C-12,14,15,17	H-15,17	H-16
17	127.7 (d)	17	7.74 (2H, m)	C-3,12,13,16	H-16	H-17
12′	132.6 (s)	–	–	–	–	–
13′	135.2 (s)	–	–	–	–	–
14′	130.3 (d)	14′	7.35 (2H, d)	C-12′,13′,15′,16′	H-15′	H-14′
15′	129.5 (t)	15′	7.40 (2H, t)	C-13′,14′,16′,17′	H-14′,16′	H-15′
16′	127.0 (t)	16′	7.34 (2H, m)	C-12′,14′,15′,17′	H-15′,17′	H-16′
17′	127.7 (d)	17′	7.74 (2H, m)	C-9,12′,13′,15′	H-16′	H-17′

Table 2
^{1}H and ^{13}C NMR chemical shifts, υ (ppm), multiplicities and coupling constants, J (H–H) (Hz), ^{1}H–^{1}H and ^{1}H–^{13}C correlations in HMBC, COSY and HSQC spectra for compound **2**.

C	δC (ppm)	H	δH (ppm)	HMBC	COSY	HSQC
1	70.7 (t)	1	e 3.83 (2H, d, J = 11.65 Hz) a 3.65 (2H, d, J = 11.65 Hz)	C-3,5,6,7,11	H_a-1, H_e-5 H_e-1	H_a-1, H_e-1
3	99.4 (d)	3	5.43 (2H, s)	C-1,5,13,17	–	H-3
5	71.3 (t)	5	e 4.83 (2H, d, J = 11.65 Hz) a 3.84 (2H, d, J = 11.65 Hz)	C-1,3,6,-7,11	H_a-5, H_e-1 H_e-5	H_a-5, H_e-5
6	32.5 (s)	–	–	–	–	–
7	71.3 (t)	7	e 4.83 (2H, d, J = 11.65 Hz) a 3.84 (2H, d, J = 11.65 Hz)	C-1,5,6,9,11	H_a-7, H_e-11 H_e-7	H_a-7, H_e-7
9	99.4 (d)	9	5.43 (2H, s)	C-7,11,13′,17′	–	H-9
11	70.7 (t)	11	e 3.83 (2H, d, J = 11.65 Hz) a 3.65 (2H, d, J = 11.65 Hz)	C-1,5,6,7,9	H_a-11, H_e-7 H_e-11	H-11
12	132.6 (s)	–	–	–	–	–
13	135.2 (s)	13	7.50 (4H, d)	C-3,12,14,17	H-14	H-13
14	130.3 (d)	–	–	–	–	–
15	129.5 (d)	15	7.31 (2H, m)	C-13,14,16,17	H-16	H-15
16	127.0 (d)	16	7.33 (2H, m)	C-12,14,15,17	H-15,17	H-16
17	127.7 (d)	17	7.36 (2H, d)	C-3,12,13,16	H-16	H-17
12′	132.6 (s)	–	–	–	–	–
13′	135.2 (s)	13′	7.50 (2H, s)	C-9,12′,14′,17′	H-14′	H-13′
14′	130.3 (d)	–	–	–	–	–
15′	129.5 (t)	15′	7.31 (2H, m)	C-13′,14′,16′,17′	H-16′	H-15′
16′	127.0 (t)	16′	7.33 (2H, d)	C-12′,14′,15′,17′	H-15′,17′	H-16′
17′	127.7 (d)	17′	7.36 (2H, d)	C-9,12′,13′,15′	H-16′	H-17′

Table 3
^{1}H and ^{13}C NMR chemical shifts, υ (ppm), multiplicities and coupling constants, J (H–H) (Hz), ^{1}H–^{1}H and ^{1}H–^{13}C correlations in HMBC, COSY and HSQC spectra for compound **3**.

C	δC (ppm)	H	δH (ppm)	HMBC	COSY	HSQC
1	70.5 (t)	1	e 3.82 (2H, dd, J = 11.5 Hz, J = 2.5 Hz) a 3.65 (2H, d, J = 11.5 Hz)	C-3,5,6,7,11	H_a-1, H_e-5 H_e-1	H_a-1, H_e-1
3	101.5 (d)	3	5.43 (2H, s)	C-1,5,13,17	–	H-3
5	71.0 (t)	5	e 4.82 (2H, dd, J = 11.5 Hz, J = 2.5 Hz) a 3.83 (2H, d, J = 11.5 Hz)	C-1,3,6,7,11	H_a-5, H_e-1 H_e-5	H_a-5, H_e-5
6	32.5 (s)	–	–	–	–	–
7	71.0 (t)	7	e 4.82 (2H, dd, J = 11.5 Hz, J = 2.5 Hz) a 3.83 (2H, d, J = 11.5 Hz)	C-1,5,6,9,11	H_a-7, H_e-11 H_e-7	H_a-7, H_e-7
9	101.5 (d)	9	5.4 3 (2H, s)	C-7,11,13′,17′	–	H-9
11	70.5 (t)	11	e 3.82 (2H, dd, J = 11.5 Hz, J = 2.5 Hz) a 3.65 (2H, d, J = 11.5 Hz)	C-1,5,6,7,9	H_a-11, H_e-7 H_e-11	H_a-11, H_e-11
12	134.9 (s)	–	–	–	–	–
13	127.5 (d)	13	7.42 (4H, d, J = 8.5 Hz)	C-3,12,14,17	H-14	H-13
14	128.5 (d)	14	7.35 (4H, d, J = 8.5 Hz)	C-12,13,15,16	H-13	H-14
15	136.4 (s)	–	–	–	–	–
16	128.5 (d)	16	7.35 (4H, d, J = 8.5 Hz)	C-12,14,15,17	H-17	H-16
17	127.5 (d)	17	7.42 (4H, d, J = 8.5 Hz)	C-3,12,13,16	H-16	H-17
12′	134.9 (s)	–	–	–	–	–
13′	127.5 (d)	13′	7.42 (4H, d, J = 8.5 Hz)	C-9,12′,14′,17′	H-14′	H-13′
14′	128.5 (d)	14′	7.35 (4H, d, J = 8.5 Hz)	C-12′,13′,15′,16′	H-13′	H-14
15′	136.4 (s)	–	–	–	–	–
16′	128.5 (d)	16′	7.35 (4H, d, J = 8.5 Hz)	C-12,14,15,17	H-17′	H-16′
17′	127.5 (d)	17′	7.42 (4H, d, J = 8.5 Hz)	C-9,12′,13′,15′	H-16′	H-17′

was constructed by intermolecular weak interaction including Cl···HAr and CH···π, respectively (Fig. 3).

3.3. Crystal X-ray diffraction guided assignment of protons in four methylenes of 3,9-di(o-chlorophenyl)-2,4,8,10-tetraoxaspiro[5.5]undecane **1** in ^{1}H NMR spectrum

Use **1** as a model compound to determine the ^{1}H NMR signals for the four methylenes. As depicted in Fig. 2 and partial ^{1}H NMR spectrum of compounds **1** in Fig. 4, firstly, the H-5(7) in "methylene inside" oriented toward the other 1,3-dioxane ring are more deshielded than H-1(11) in "methylene outside" oriented in opposite direction as a result of the influence of the van der Waals Radii site effect induced by oxygen atoms of the different six-member heterocycles [5], so the signals of H-5(7) (4.95 ppm and 3.95 ppm) are in lower field than H-1(11) (3.88 ppm and 3.75 ppm). Secondly, for positions 5(7), the equatorial protons (H_e) are closer to different ring oxygens than the axial ones (H_a), so the former is more deshielded than the latter [H_e-5(7) *vs* H_a-5(7), 4.95 ppm *vs* 3.95 ppm]. In the case of 1(11), the signal of H_e-1(11) (3.88 ppm) are in lower field than that of H_a-1(11) (3.75 ppm) result from the anisotropic effects of single bonds in the six-member heterocycles [12,17]. Finally, the equatorial protons [H_e-5(7) and H_e-1(11)] on the same plan can further split to form the double-double peaks [4.95 (2H, dd, J = 11.5 Hz, J = 2.5 Hz) and 3.88 (2H, dd, J = 11.5 Hz, J = 2.5 Hz)] due to coupling of the two terminal protons on W disposal involving four bonds [18,23]. Moreover, all the ^{1}H NMR signal assignments of methylenes of compound **1** were in agreement with the corresponding data of ^{13}C NMR, DEPT, ^{1}H-^{1}H COSY, HSQC, and HMBC (Table 1).

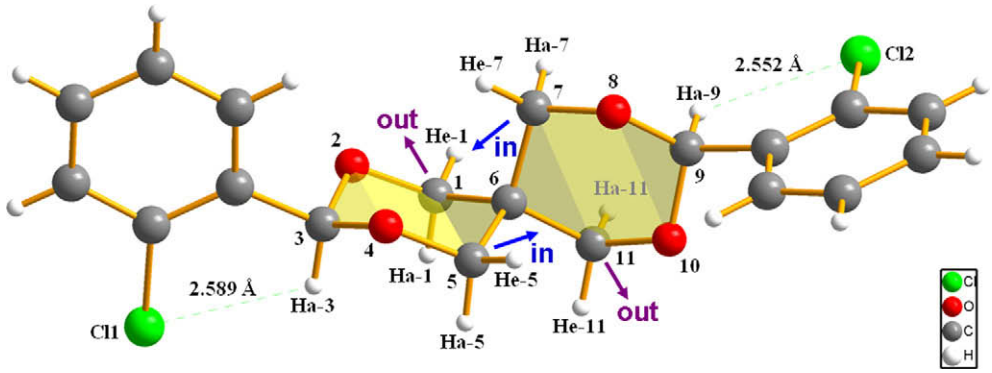

Fig. 2. Crystal structure of compound **1**.

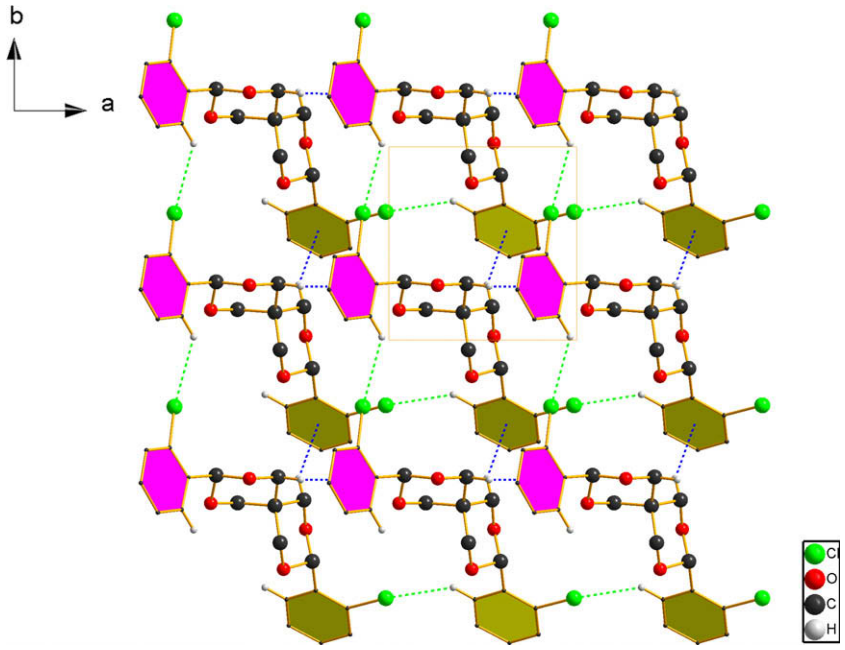

Fig. 3. The molecular packing along *a* and *b* axis in the crystal structure of **1** (dashed lines indicate Cl···HAr (green) and CH···π (blue) weak interactions). (For interpretation of the references to colour in this figure legend, the reader is referred to the web version of this article.)

*3.4. Crystal structure guided NMR analysis for compounds **1–3** under differently shielding effect of terminal aromatic rings*

With the unambiguous NMR signal assignment for compound **1** in hand, different substrates **2** and **3** were further probed to illustrate the influence on NMR induced by differently shielding effect of terminal aromatic rings. As shown in Fig. 4, despite of unique discrimination among the three isomers **1–3** caused by different positions of the chlorine atoms on the aromatic rings, obviously different signals including the chemical shifts and split pattern of protons in two six-member heterocycles were observed. The signals of H-5(7), H-1(11) and H-3(9) were similar in compounds **2** and **3**, while those of the compound **1** gave great difference. It might be attributed to the different steric structure and electronic effect of aryl resulted from chlorine atom located at different positions on benzene rings. Firstly, there are weak interactions between H-3(9) and Cl1(2) in compound **1** (distance of CH···Cl, 2.589 Å and 2.552 Å, Fig. 2) while none in compounds **2** and **3** because of the long distance between H-3(9) and Cl1(2). It conducted that the H-3(9) signal in compound **1** shifted 0.41 ppm toward low field comparing with that in the compounds **2** and **3**. Secondly, owing to the differently shielding effects of aromatic rings, four methylenes proton signals in compound **1** shifted about 0.1 ppm toward low field and the corresponding carbon signals also gave rise to downfield shifts (Tables 1–3) than those of compounds **2** and **3**. Moreover, in compounds **2** and **3**, four groups of peaks of methylenes were not completely separated, the signals of H_a-5(7) and H_e-1(11) partially overlapped, and their chemical shifts moved toward high field contrasting to compound **1**. These phenomena indicated that the terminal aromatic rings could significantly affect the chemical shifts and split pattern of hydrogens and carbons in six-member heterocycles of 3,9-diaryl-2,4,8,10-tetraoxaspiro[5.5] undecanes. Although the effect of different brominated alkyl [13], alkyl and phenyl [12] on position 3,9 of 2,4,8,10-tetraoxaspiro[5.5]undecanes have been described by Grosu, it is the first time that the influence of aryl bearing different steric and electronic effect was discussed here.

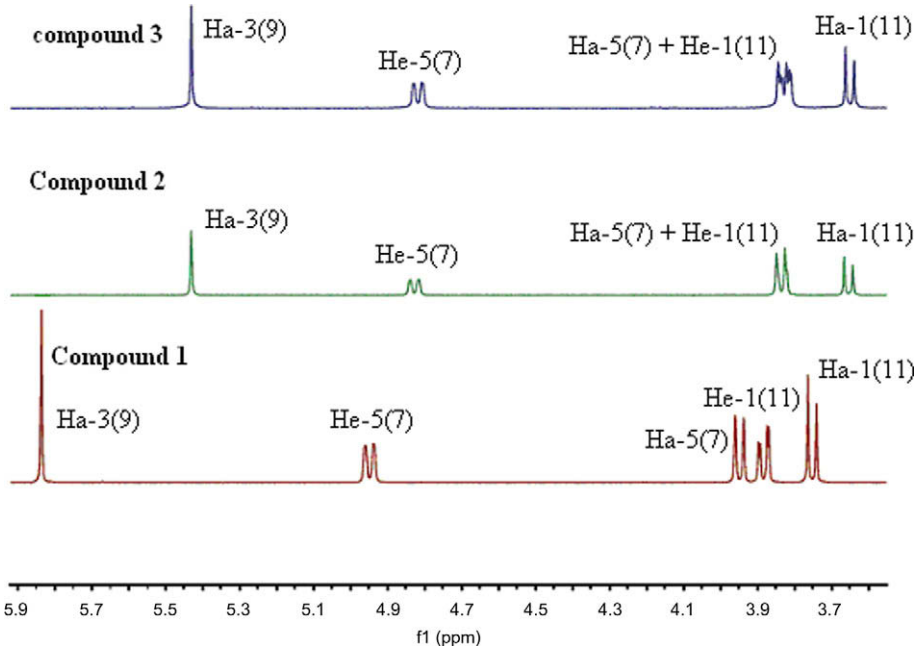

Fig. 4. The partial ^{1}H NMR spectra of compounds **1**–**3**.

4. Conclusion

We have completely and accurately assigned all the proton and carbon signals for 3,9-di(*o*-, *m*- and *p*-chlorophenyl)-2,4,8,10-tetraoxaspiro[5.5]undecanes **1–3** by using 1D and 2D NMR techniques including ^{1}H, ^{13}C NMR, DEPT135, ^{1}H-^{1}H COSY, HSQC, and HMBC experiments. The NMR analysis guided by crystal X-ray diffraction disclosed that despite of the same environment of the two six-member rings, the chemical environment of two methylenes existing in the same ring and the two protons in the same methylene were both different because of the molecular axial chirality. Furthermore, the chemical shifts and split pattern of hydrogens and carbons in two six-member heterocycles could be influenced by the location of substituent on the terminal aromatic rings. This study has provided significant proofs for the identification of the similar structures as pentaerythritol diacetals bearing spiro-1,3-dioxanes skeleton.

Acknowledgement

We gratefully acknowledge financial support from the Natural Science Foundation of China (No. 20872051).

References

[1] C. Cismaş, A. Terec, S. Mager, I. Grosu, Curr. Org. Chem. 9 (2005) 1287.
[2] A. Mihiş, E. Condamine, E. Bogdan, A. Terec, T. Kurtán, I. Grosu, Molecules 13 (2008) 2848.
[3] I.G. Mursakulov, E.A. Ramazanov, M.M. Guseinov, N.S. Zefirov, V.V. Samoshin, E.L. Eliel, Tetrahedron 36 (1980) 1885.
[4] H. Dodziuk, J. Chem. Soc., Perkin Trans. 2 (1986) 249.
[5] H. Dodziuk, J. Sitkowski, I. Stefanian, I.G. Mursakulov, M.M. Guseinov, V.A. Kurbanova, Struct. Chem. 3 (1992) 269.
[6] I. Grosu, S. Mager, G. Plé, M. Horn, J. Chem. Soc. Chem. Commun. (1995) 167.
[7] I. Grosu, S. Mager, G. Plé, J. Chem. Soc., Perkin Trans. 2 (1995) 1351.
[8] I. Grosu, S. Mager, G. Plé, E. Mesaros, Tetrahedron 52 (1996) 12783.
[9] D. Opris, I. Grosu, L. Toupet, G. Plé, A. Terec, S. Mager, L. Muntean, J. Chem. Soc., Perkin Trans. 1 (2001) 2413.
[10] A. Terec, I. Grosu, E. Condamine, L. Breau, G. Plé, Y. Ramondenc, F.D. Rochon, V. Peulon-Agasse, D. Opris, Tetrahedron 60 (2004) 3173.
[11] N.G. Lemcoff, B. Fuchs, Org. Lett. 4 (2002) 731.
[12] S. Mager, M. Horn, I. Grosu, M. Bogdan, Monatsh. Chem. 120 (1989) 735.
[13] I. Grosu, S. Mager, G. Plé, R. Martinez, M. Horn, R.R. Gavino, Monatsh. Chem. 126 (1995) 1021.
[14] M.J.O. Anteunis, D. Tavernier, F. Borremans, Heterocycles 4 (1976) 293.
[15] E. Mesaros, I. Grosu, S. Mager, G. Plé, I. Farcas, Monatsh. Chem. 129 (1998) 723.
[16] H. Jiang, S.J. Tu, X.Y. Liu, J.S. Yang, Y.J. Feng, Chin. J. Magn. Reson. 3 (2006) 333.
[17] T. Tan, NMR in Organic Chemistry, High Education, Beijing, 1998.
[18] S. Xue, Organic Structural Analysis, Chinese Science and Technology, Hefei, 2005.
[19] G.M. Sheldrick, SHELXS-97: Program for Crystal Structure Solution, University of Göttingen, Göttingen, 1997.
[20] G.M. Sheldrick, SHELXL-97: Program for Crystal Structure Refinement, University of Göttingen, Göttingen, 1997.
[21] J.-K. Wang, D.-Y. Yan, L.-J. Liu, S. Liu, J.-T. Wang, Acta Cryst. E62 (2006) o3062.
[22] M.A. Khusainov, S.S. Makarevich, A.E. Obodovskaya, Z.A. Starikova, R.S. Musavirov, Zh. Strukt. Khim. 29 (1988) 154.
[23] H. Günther, NMR Spectroscopy, second ed., Wiley, Chichester, 1995.